

Learning Robust Penetration-Testing Policies under Partial Observability: A systematic evaluation

Raphael Simon^{1,2}, Pieter Libin^{*2}, and Wim Mees^{*1}

¹CISS Department, Royal Military Academy

²Artificial Intelligence Lab, Vrije Universiteit Brussel

Abstract

Penetration testing, the simulation of cyberattacks to identify security vulnerabilities, presents a sequential decision-making problem well-suited for reinforcement learning (RL) automation. Like many applications of RL to real-world problems, partial observability presents a major challenge, as it invalidates the Markov property present in Markov Decision Processes (MDPs). Partially Observable MDPs require history aggregation or belief state estimation to learn successful policies. We investigate stochastic, partially observable penetration testing scenarios over host networks of varying size, aiming to better reflect real-world complexity through more challenging and representative benchmarks. This approach leads to the development of more robust and transferable policies, which are crucial for ensuring reliable performance across diverse and unpredictable real-world environments. Using vanilla Proximal Policy Optimization (PPO) as a baseline, we compare a selection of PPO variants designed to mitigate partial observability, including frame-stacking, augmenting observations with historical information, and employing recurrent or transformer-based architectures. We conduct a systematic empirical analysis of these algorithms across different host network sizes. We find that this task greatly benefits from history aggregation. Converging three times faster than other approaches. Manual inspection of the learned policies by the algorithms reveals clear distinctions and provides insights that go beyond quantitative results.

Keywords— Penetration Testing, Reinforcement Learning, Partial Observability

1 Introduction

The world is more interconnected than ever. Dependence on this connectivity has become deeply ingrained in our society. Never before have so many computer systems been deployed to operate our critical infrastructure, such as health, finance, transportation and energy. At the same time, cyber-related threats continue to grow,

^{*}Equal contribution, alphabetical order.

posing significant risks, especially for these critical infrastructures [27, 53]. Defending those systems is a significant challenge, especially given the fundamental asymmetry; defenders have to cover every possible security flaw while attackers often only need a single point of entry. One way to strengthen the security posture of companies and organizations is to perform penetration testing and red teaming, in which ethical hackers try to uncover vulnerabilities or implement specific techniques and procedures to emulate advanced adversaries, such as nation-state-sponsored actors [25]. This allows defenders to uncover blind spots in their detection capabilities and be better prepared for future attacks. It also enables them to practice and refine their responses in case of a real attack. Conducting these security assessments requires experienced professionals, who are in short supply [18], and the process is time-consuming and costly. In their work, penetration testers use numerous tools the community has developed, which allow for some automation of the work. However, automation of the overall process remains an unresolved challenge, yet is crucial to help professionals scale their efforts to secure more systems and protect critical infrastructure.

The key difficulty lies in decision-making: skilled practitioners must continuously evaluate partial information, adapt to dynamic network conditions, and choose from a vast array of possible actions. These sequential decision-making challenges, involving long-term consequences, are well-suited to formulation as reinforcement learning (RL) problems. RL’s ability to learn optimal behaviour through trial and error makes it particularly suited for penetration testing. Just as human penetration testers (or pentesters) learn to improve their strategies through experience, RL agents learn policies that balance immediate rewards with long-term outcomes, optimizing cumulative performance over time [47]. This parallel becomes particularly compelling with the emergence of Deep Reinforcement Learning (DRL), which has achieved superhuman performance in complex strategic environments, from mastering Atari games [28] to pioneering self-play approaches in competitive domains like Dota [5] and Go [44]. Further successes in complex real-world applications include the design of a magnetic controller for nuclear fusion in a tokamak configuration [9] to learning prevention strategies in the context of pandemic influenza [26]. Inspired by these achievements, researchers have started applying DRL to automate the penetration testing process.

Several environments have been proposed in the literature to enable both the simulation of penetration testing and facilitating the training of RL agents [19, 32, 43, 45, 48]. Learning directly in real-world environments remains an outstanding challenge, not only due to the sample inefficiency of RL algorithms [11], but also the time cost of resetting virtualized infrastructure for each episode. Regarding the training of agents in simulated environments, we find that most of the work formalises the problem of penetration testing as a Markov Decision Process, allowing the agent to perceive the full state of the environment [21, 50, 57]. While this assumption may be reasonable in certain scenarios, it has long been criticized as an oversimplification of real-world conditions, for penetration testing, where information gathering is a core component of the task [40]. Framing the problem as partially observable requires the agent to seek information, evaluate it, and then act accordingly, mimicking human penetration testers. Another challenge current methods are facing is overfitting [7, 55], where agents learn the training environment by heart and as such do not generalise to previously unseen scenarios. In the context of penetration testing, learning policies that are applicable to multiple network configurations is a crucial step toward achieving robustness and real-world applicability.

To address these challenges, this work formalizes the network penetration testing task as a partially observable and stochastic decision-making problem. Since existing environments do not highlight these challenges sufficiently, we make the necessary adaptations to the Network Attack Simulator (NASim) and provide a new environment we call StochNASim. First, we add stochasticity related to the network topology by generating a new permutation of the network every episode. The hosts will be re-

generated and have new properties such as which processes, services and operating system (OS) they are running. Second, we enlarge the observation space to account for different network sizes. As a result, the agent will have to act successfully in an environment composed of 5 hosts in one episode, while in the next episode it might encounter a network of 8 hosts. This increases the number of possible observations the agent perceives, rendering the environment more challenging. It also highlights the challenge to learn a policy that effectively generalizes. Using this environment, we evaluate distinct techniques for addressing partial observability that have shown promise in prior DRL applications. Our selection includes frame stacking and observation augmentation, as well as more expressive architectures such as recurrent neural networks and transformers. We compare all methods against vanilla PPO as a baseline, which has no specific mechanism for handling partial observability. To ensure a fair comparison, we conduct a comprehensive hyperparameter search for each algorithm and verify these hyperparameter sets on several control seeds to assure their robustness. Through this systematic evaluation, we seek to better understand effective strategies for addressing partial observability and stochastic dynamics in the context of automated penetration testing.

We summarize our contributions as follows:

1. We adapt NASim to create StochNASim, a new partially observable and stochastic penetration testing environment with variable network sizes that better reflects real-world challenges and allows the learning of robust and transferable policies.
2. We conduct a systematic empirical evaluation of different approaches for handling partial observability in penetration testing scenarios.
3. We demonstrate that simple observation augmentation can significantly outperform complex architectures (LSTMs, transformers), challenging conventional assumptions about memory mechanisms in this domain.
4. We provide comprehensive policy analysis through action sequence visualization, revealing qualitative differences between algorithmically similar solutions that go beyond quantitative performance metrics.

2 Background

2.1 Markov Decision Processes

Markov Decision Processes (MDPs) are a class of stochastic sequential decision processes in which the cost and transition functions depend only on the current state of the system and the current action [36]. An MDP is formalized as a tuple $\langle \mathcal{S}, \mathcal{A}, \mathcal{P}, \mathcal{R}, s_I, \gamma \rangle$ where \mathcal{S} is the set of all *states* the environment can take upon; \mathcal{A} a set of *actions* that can be executed in the environment; $\mathcal{P}(s'|s, a)$, the transition probability distribution over next states, conditioned on the current state and action; $\mathcal{R}(s, a) \rightarrow \mathbb{R}$, a reward function; $s_I \in \mathcal{S}$, the initial state, which can itself be a distribution; and $\gamma \in [0, 1]$ a discount factor, that signifies the importance of future rewards. MDPs are characterized by the Markov property: given the current state, the future is independent of the past. The objective in an MDP is to learn a policy $\pi(a|s)$, a probability distribution over actions conditioned on the current state, that maximizes the expected cumulative discounted reward $G_t = \mathbb{E}_\pi[\sum_{t=0}^{\infty} \gamma^t r_t]$, which we call the return, and where r_t is a random variable that represents the reward obtained at time step t . In finite-horizon tasks the sum is clipped to T , the maximum number of allowed steps.

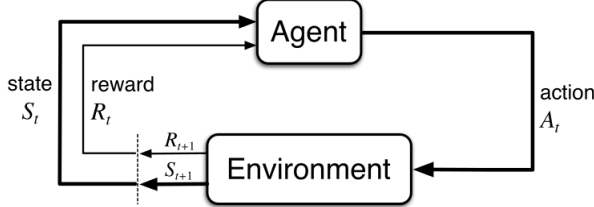


Figure 1: The agent–environment interaction in reinforcement learning. Adapted from [47].

2.2 Partially Observable Environments

In many real-world scenarios, the true state of the environment cannot be observed, necessitating the framework of Partially Observable Markov Decision Processes (POMDPs). A POMDP extends the MDP framework to a tuple $\langle \mathcal{S}, \mathcal{A}, \mathcal{P}, \mathcal{R}, \Omega, \mathcal{O}, s_I, \gamma \rangle$, where Ω represents the observation space and $\mathcal{O}(o|s', a)$ defines the observation function. In POMDPs, the Markov property holds for the hidden states, but not for the observations, which provide only partial information about the environment. Therefore, the agent must maintain a belief state $b_t(s)$, representing a probability distribution over possible states at time t . The optimal policy must now map beliefs to actions: $\pi(a|b)$.

2.3 Reinforcement Learning

Reinforcement Learning (RL) provides a general framework for learning optimal behavior in MDPs and POMDPs through interaction with an environment [47]. An RL agent learns from experience rather than requiring a complete model of the environment. At every time step t , the agent in state $s_t \in \mathcal{S}$ picks an action $a_t \in \mathcal{A}$. It then receives a reward r_{t+1} for the outcome of that action, and perceives the new state s_{t+1} . This interaction loop is depicted in Figure 1.

For MDPs, common RL approaches include value-based methods (e.g., Q -learning), policy gradient methods, and hybrid actor-critic algorithms, each with distinct trade-offs in sample efficiency, computational complexity, and suitability for discrete or continuous action spaces. Value functions estimate how good it is for an agent to be in a given state. The value function is defined as: $V_\pi(s) \doteq \mathbb{E}[G_t|s_t = s]$. It tells us the value of the state the agent is in at time step t when following policy π from there onwards. Another commonly used value function is the Q -function, or the state-action value function: $Q_\pi(s, a) \doteq \mathbb{E}[G_t|s_t = s, a_t = a]$. It defines the value of being in state s at time step t , taking action a , and following the policy π from there onwards.

For POMDPs, RL approaches typically incorporate mechanisms to handle partial observability. These include belief state computation [20] and recurrent neural networks (RNNs) to implicitly encode the history [13]. Recent advances have explored attention mechanisms and transformer architectures to better capture long-term dependencies in observation history [33, 35].

2.4 Penetration Testing

Penetration testing (pentesting) is a systematic cybersecurity methodology where security professionals simulate adversarial attacks against information systems. The goal is to identify, exploit, and document security vulnerabilities before malicious actors can leverage them. This practice is integral to an organization’s security assessment program and defence strategy. The typical pentesting workflow includes: (1) Reconnaissance and information gathering to map the target environment; (2) Vulnerability

scanning and analysis to identify potential security weaknesses; (3) Perform exploitation attempts to confirm vulnerability exploitability; (4) Post-exploitation activities to assess potential impact and privilege escalation paths; and (5) Documentation of findings and remediation recommendations [29].

Penetration testing methodologies vary based on the level of prior knowledge provided to the tester. In white-box testing, testers receive comprehensive system information, including network architecture, source code, and configuration details. Black-box testing provides minimal information, simulating an external threat actor’s perspective. Gray-box testing represents an intermediate approach, offering partial internal knowledge to simulate insider threats or advanced persistent threats that have already gained limited access [30].

The sequential decision-making nature of penetration testing makes it particularly suited for automation through RL. Network topologies may be only partially discovered, and the success of exploitation attempts may depend on unpredictable factors. These characteristics require agents to make decisions with incomplete information about the environment state. The challenge of partial observability and stochasticity is especially pronounced in black-box and gray-box testing scenarios, where information collection becomes an integral part of the procedure [40].

3 Related Work

Several simulation environments have been developed to enable RL research in penetration testing, each with different design choices regarding scope and complexity. NASim [43] provides configurable penetration testing scenarios through configuration files and supports both full and partial observability modes. CybORG [45] was designed as an AI Gym for autonomous cyber operations, supporting both offensive and defensive agents while offering partial observability options. CyberBattleSim [48] focuses specifically on lateral movement and privilege escalation rather than full penetration testing workflows, using a node-based simulation with detailed network configurations.

More recent environments have built upon these foundations. NASimEmu [19] extends NASim with an emulation component to enable evaluation in more realistic settings, while Cyberwheel [32] supports both red and blue team operations with actions mapped to the MITRE ATT&CK framework [46].

While these environments provide partial observability capabilities, most subsequent research has opted for the simpler fully observable formulation [21, 22, 50, 54, 57]. This preference for full observability is justifiable, given the additional complexity and difficulty of achieving good performance under partial observability. However, this trend has left a significant gap in understanding how different approaches handle the information-gathering challenges inherent in real-world penetration testing. Additionally, existing evaluations typically use fixed network topologies, limiting the assessment of policy generalization. These factors motivate this study: we systematically compare partial observability methods in StochNASim, our adaptation of NASim that combines partial observability with stochastic network generation to better reflect real-world challenges.

Several recent works have begun to address partial observability in automated penetration testing. The dominant approach has been to augment RL algorithms with recurrent architectures. Zhang et al. combine Double DQN with LSTM [56], while Li et al. propose EPPTA, replacing PPO’s feedforward networks with RNNs [24]. Ren et al. follow the same principle, also adding an LSTM architecture to PPO, but additionally incorporate an intrinsic curiosity module to help with exploration [39].

Terranova et al. initially formulate penetration testing as a POMDP but acknowledge that standard DRL algorithms struggle with high partial observability [49].

To address this, they augment the observation space with historical information (e.g., previously exploited vulnerabilities), effectively transforming the POMDP into an augmented MDP, which is easier to solve. Beyond RNN approaches, Li et al. incorporate reward machines (RM), a form of [23]. Reward machines allow encoding of domain knowledge by providing intermediate rewards when the agent transitions between pre-defined states within the machine state machine [17]. The authors implement two reward machines representing different preferences and compare Q-learning with reward machines to standard DQN.

However, these works typically compare against limited baselines and lack a systematic evaluation of different approaches on handling partial observability across varying network configurations. They also fail to compare expensive-to-train RNN-based methods against simpler alternatives like observation augmentation or frame stacking.

4 Methodology

First, we present a formalisation of our environment. Next, we discuss the different algorithms that have been selected to address the presented issues. Finally, we provide a detailed overview of our hyperparameter search procedure.

4.1 Environment

In this work, we extend the Network Attack Simulator (NASim) [43]. NASim simulates a network of hosts organized into subnets—logical subdivisions that group connected devices based on network requirements. Firewalls are positioned between subnets to control traffic flow, either allowing or blocking communication in specific directions. In this environment, the goal is to obtain root privileges on two hosts marked as *sensitive*. This is analogous to real-world exercises, where some hosts are more important than others. Reasons for classifying some hosts as sensitive include: containing sensitive data, or serving as major gateways into other network segments.

We chose to extend this simulator because it provides a good balance of realism and computational efficiency, offers a simple yet flexible framework, and captures the key challenges of penetration testing. What we found lacking was the ability to train on permutations of the same network configuration, which is required for testing algorithms’ capabilities for learning in stochastic environments and evaluating how well policies generalize. To address this limitation, we extended the environment to support networks of variable size to add additional complexity. We now formalise the environment, which we call StochNASim, and describe all the important components and modifications we introduced to investigate algorithms for learning policies in partially observable and stochastic networks of variable size.

State

The overall network state is defined by the collective states of all individual hosts within it. A *host vector* encodes all the information about a particular host. The shape of the network state is a matrix of shape $m_c \times n$, where m_c is the current number of hosts in the generated network and n is the length of the host vector. The features of a host, as encoded in the host vector, are:

1. Subnet address: one-hot encoding with length equal to the maximum number of subnets possible in the network.
2. Host address: one-hot encoding with length equal to the maximum number of hosts in any subnet.

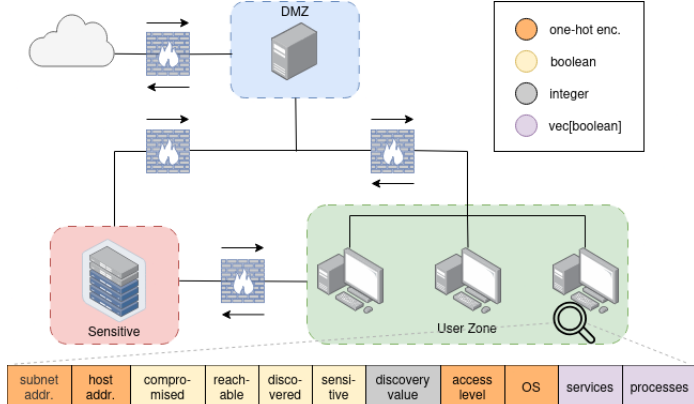


Figure 2: Example network topology in StochNASim showing five hosts across different security zones. The diagram illustrates key host properties including subnet membership (DMZ, User Zone, Sensitive), operating systems, running services, and access levels.

3. Compromised (**boolean**), reachable (**boolean**), discovered (**boolean**), sensitive (**boolean**).
4. Discovery value (**float**): reward to receive upon discovering this host.
5. Access level: a one-hot encoding of the access level of the host. We consider three different access levels: *no access currently, user, root*.
6. Operating System (OS): a one-hot encoding of every OS in the configuration.
7. Services running (**vec[boolean]**): representing each service running on the host.
8. Processes running (**vec[boolean]**): representing each process running on the host.

An example network with host properties is showcased in Figure 2. When an agent interacts with the environment, only four host values can change: *compromised, reachable, discovered*, and *access level*. All other values remain static after the environment is generated. The agent's perceived state includes the state matrix, plus four action outcome flags: action success, connection error, permission error, and undefined error. This additional information is padded with zeros to match the host vector length and added as a new row to the state matrix. As a result, the information fed to the agent is of the shape $(m_c + 1) \times n$.

Initial State

The initial state determines the position of every host within the network, including whether they are compromised, reachable, discovered, sensitive, and their current access level. It also encodes the OS, services, and processes running on each host. When the network is generated, every host is assigned a subset of running services and processes. Specifically, from the set of all available services \mathbb{S} and processes \mathbb{P} , each host runs n_s services and n_p processes, where $n_s < |\mathbb{S}|$ and $n_p < |\mathbb{P}|$. Assigning only a subset of the total available services and processes to hosts is to make exploitation more difficult, requiring the agent to carefully investigate the host before selecting the action. Due to using a variable number of hosts and generating them anew, StochNASim has a distribution of initial states instead of a stationary initial state like in NASim. The agent starts on one host at the edge of the network. We note that

the agent remains stationary in the network topology, acquiring deeper access to hosts rather than navigating between them.

Actions

The environment contains seven different action types:

- **Exploit:** Exploit a vulnerable service (i.e., perform remote exploitation). Each exploit action targets a specific service and OS combination. To successfully exploit a host, it needs to run the targeted service and OS. If the exploit succeeds, we earn the access level that it provides on that host.
- **Privilege Escalation:** Exploit a vulnerable process (i.e., perform local exploitation). Similar to the exploits, privilege escalation actions need a specific OS and process pair to run successfully.
- **Service Scan:** Scan a host for its services.
- **Process Scan:** Scan a host for its processes.
- **OS Scan:** Scans a host for its OS.
- **Subnet Scan:** Scans the subnet the host belongs to.
- **No Op:** Do nothing.

Each action is described by the host it targets, its cost, success probability and the required access level. Exploits additionally specify the required OS and service pair they target, while privilege escalation actions specify the required OS and process pair. Finally, these actions also list which access they provide upon successful execution.

Action Space

The overall action space is constructed according to the number of hosts. For every host, there is one set of scan actions (**Service Scan**, **Process Scan**, **OS Scan**, **Subnet Scan**) which we denote **S**. To have one congruent set of actions that works against every host, we associate one exploit action for every service and OS combination, and one privilege escalation action for every process and OS. Therefore, the size of the action space is denoted as $|\mathcal{A}| = \lceil H \rceil \times (|\mathbf{S}| + |OS| \times (|S| + |P|))$ where H is the number of hosts, S is the number of services per host, and P the number of processes per host configured in the environment.

Observations

In the partially observable case we consider, the observations that are perceived by the agent only contain the direct result of each action. For instance, if we scan host h_3 for its OS, then we only get back that information, plus the host's address. Each successful action $a \in \mathcal{A}$ yields a different observation, which together form the observation space Ω . To allow for variable-sized networks, we use observation sizes of $(m + 1) \times n$, where m is the maximum number of hosts considered and $m_c \leq m$.

Transition Function

To transition from one state to another, the agent needs to execute actions. Scan actions are deterministic, while **Exploit** and **Privilege Escalation** actions have a success probability p assigned to them, following a Bernoulli distribution. State transitions occur when actions succeed based on this probability and when all necessary preconditions are met. These preconditions are:

- Each action requires that the target host is reachable.

- The **Process Scan** requires a *user* access level to succeed, while the **Subnet Scan** requires *root* privileges.
- When performing an **Exploit** or **Privilege Escalation** action, the target host must run the respective service or process that is targeted by that action.
- Additionally, **Privilege Escalation** requires the *user* access level on the host. This implies that first, a successful **Exploit** is required to gain the necessary access.
- Once an action has been successfully executed, repeating it has no further effect on the state.

Network Generation

NASim’s network generation procedure creates penetration testing scenarios with a structured topology that mimics real-world enterprise networks. The generator allocates hosts across multiple subnets following a specific formula: for every 40 hosts in the network, one is assigned to the DMZ subnet, one to the Sensitive subnet, and the remainder are distributed among User subnets (with 5 hosts per subnet at most). This creates a hierarchical structure with an Internet subnet (1 host), DMZ, Sensitive, and User subnets arranged in a binary tree topology. Each host is configured with an OS, a subset of available services, and a subset of available processes. To ensure the network presents a viable penetration testing challenge, the generator guarantees exploitable paths to sensitive hosts through three mechanisms: ensuring each subnet contains at least one vulnerable host, making all sensitive hosts vulnerable to root-level access, and configuring firewall rules to allow at least one vulnerable service between network zones. The generator creates exploit actions for each OS-service combination and privilege escalation actions for each OS-process combination, ensuring that attackers can chain together exploits to traverse the network topology and ultimately compromise the sensitive hosts.

Rewards

The reward function is defined by Equation 1. The value of hosts is denoted by V_h . By scanning the subnet, new hosts can be discovered. The value of discovering a host is denoted by V_d . The reward is multiplied by the number of *newly* discovered hosts, n_{dh} . Hosts may only be discovered once. In all other scenarios, the returned reward is the cost of the action a_t .

$$r_t = \begin{cases} -\text{cost}(a_t) + V_d \times n_{dh} & \text{for successful} \\ & \text{subnet scans,} \\ -\text{cost}(a_t) + V_h & \text{for successful} \\ & \text{priv. esc.,} \\ -\text{cost}(a_t) & \text{else.} \end{cases} \quad (1)$$

Stochasticity

We argue that introducing additional stochasticity is crucial in the domain of penetration testing, as it enables learning more robust policies applicable to a diverse range of networks with varying services and processes, rather than policies that overfit to a single network configuration. By default, the only stochasticity in the original environment is the success probability of actions. To enable learning in such a challenging scenario, we have extended NASim in several key areas, creating what we call StochNASim. Our modifications include: First, we extended the observation space to accommodate a maximum of m hosts, representing the upper-bound of our variable

network scenarios. Second, we generate a new network upon each environment reset, effectively sampling a new initial state $s_I \subset \mathcal{S}$. While the number of current hosts m_c remains within defined bounds, the specific services and processes running on each host are regenerated with each reset. Third, we regenerate the action space with each reset to align with the initial state, to ensure a set of valid actions. While the target host address (subnet, host number) changes to match the current network configuration, all other action properties remain consistent—reflecting the stable toolbox used by real security professionals. We define one exploit action for every OS-service combination and one privilege escalation action for every OS-process combination. When the current number of hosts (m_c) is less than the maximum (m), we pad the remaining action space with `No Op` actions and return a connection error in the observation should such an action be invoked.

These modifications result in an environment that supports networks of varying sizes up to m hosts, where each reset generates a new network with hosts having different properties. The consistency in action types ensures that the agent learns to associate action a_i with its function rather than with specific network configurations, promoting generalization across different network topologies.

4.2 Algorithm Selection

We now present the selection of different algorithms and methods to address the partial observability of the StochNASim environment. Acting in POMDPs is a challenging task, and finding efficient approaches to solve them is still an active area of research [3, 12]. We focus on model-free methods that have shown success in prior research and have been applied to tasks similar to ours. Our algorithm selection encompasses both established approaches from the penetration testing literature and promising techniques from the broader POMDP research community.

Baseline

As a baseline we consider PPO. PPO is a policy gradient method, that directly optimizes the policy parameters. The policy gradient theorem provides the theoretical foundation for algorithms like REINFORCE, which update the policy parameters in the direction of the gradient $\nabla_{\theta} J(\theta)$, where $J(\theta) = \mathbb{E}_{\tau \sim \pi_{\theta}}[G_t]$ [52]. Here, τ denotes a trajectory, a sequence of states, actions and rewards. In other words, the objective is to maximize the expected return of trajectories sampled from the current policy. However, vanilla policy gradient methods suffer from high variance and poor sample efficiency.

Actor-critic algorithms address these limitations by incorporating a value function to reduce variance. Instead of using Monte Carlo returns, such methods use an advantage estimate $A(s, a) = Q(s, a) - V(s)$, combining the benefits of both value-based and policy-based learning. Trust Region Policy Optimization (TRPO) further improves upon basic actor-critic methods by constraining policy updates to prevent catastrophically large changes that could destabilize learning [41].

PPO builds on TRPO’s insights while offering a simpler, more practical implementation. Rather than explicitly constraining the trust region through second-order optimization, PPO uses a clipped surrogate objective that effectively limits policy. This clipping mechanism prevents excessively large policy updates while maintaining computational efficiency. PPO’s robustness across domains, stable training characteristics, and widespread implementation availability make it an appropriate baseline for our comparative study of partial observability approaches [42], as well as already having been used extensively in this domain [19, 24, 39, 49].

Frame-stacking

This technique was first used in the vanilla DQN paper [28] to provide temporal context through observation history. Frames refer to the game frames of Atari. Frame-stacking provides a small short-term temporal context by combining the last f_n observations with the current observation into a single input. Prior work has shown that frame-stacking works well on several partially observable tasks, and is able to achieve comparable performance to recurrent architectures [6]. So far, this method has not been applied to automated penetration testing. To enable frame-stacking, we employ the frame stack wrapper found within the sb3 library [38]. We use the last f_n frames, whereby f_n is a hyperparameter we tune: $f_n \in \{4, 8, 16, 32\}$. Going forward, we abbreviate PPO with frame-stacking as PPO-FS.

Augmented Observations

In partially observable environments, agents must retain discovered information throughout episodes to build complete state representations. The dynamics of the environment and the structure of the state allow us to retain the information that has been obtained throughout the episode, mirroring how professional penetration testers maintain detailed notes of discovered vulnerabilities, services, and system configurations throughout their assessment. In the case of RL, this lets us acquire a representation that converges to the state of the environment as the agent explores and uncovers more information during the episode. We do this by implementing a wrapper around our environment that stacks an aggregated matrix of observations below the latest observation. The aggregation matrix is obtained by applying an element-wise maximum $O_t^{aug} = \max(O_{t-1}^{aug}, O_t)$ between itself and the latest observation, O_t . At timestep t , the top part of the observation contains the latest observation and the bottom part contains the aggregation of all the observations up to and including timestep $t-1$. We depict a simplified visualisation in Equation 2. Through this we obtain an explicit representation of the history. For instance, if a host's OS is discovered at timestep 5, this information remains visible in all subsequent observations through the aggregated matrix. The reason we stack the latest observation and the augmented matrix together, and not just use the aggregation matrix as the observation, is to provide a better signal to the agent. If we only provide the aggregated history, we end up with actions that map to the same observation, which complicates the learning process. We also omit the additional information about action outcomes from the aggregated matrix to only track state information. We call these augmented observations, and use them in conjunction with PPO. Going forward, we abbreviate PPO with augmented observations as PPO-AO.

$$O_1^{aug} = \begin{bmatrix} 0 & 1 & 0 \\ 0 & 0 & 1 \\ 0 & 0 & 0 \\ 0 & 0 & 0 \end{bmatrix}, \quad O_2^{aug} = \begin{bmatrix} 1 & 0 & 0 \\ 0 & 0 & 1 \\ 0 & 1 & 0 \\ 0 & 0 & 1 \end{bmatrix}, \quad O_3^{aug} = \begin{bmatrix} 0 & 0 & 1 \\ 1 & 0 & 0 \\ 1 & 1 & 0 \\ 0 & 0 & 1 \end{bmatrix} \quad (2)$$

Recurrent Architectures

To handle the sequential nature of observations in our partially observable environment, we evaluate PPO combined with a Long Short-Term Memory (LSTM) architecture [14]. LSTMs are particularly well-suited for partially observable environments because their gated architecture enables them to maintain a compressed representation of observation history. This memory mechanism allows the agent to approximate the true environment state from partial observations, facilitating more informed action selection. Previous work has demonstrated the effectiveness of recurrent architectures in

similar settings. Hausknecht and Stone [13] showed that integrating LSTM into DQN enables learning effective policies with single-frame observations, eliminating the need for the four-frame stacking used in the original DQN. More recently, Ni et al. [31] demonstrated that recurrent model-free RL serves as a strong baseline across various POMDPs, often matching or outperforming problem-specific approaches. Following the successful application of LSTMs in penetration testing by Zhang et al. [57], Li et al. [24], and Ren et al. [39], we evaluate this established approach as a key baseline to include. We use the LSTM-based PPO variant from the `sb3-contrib` repository [38]. Going forward, we abbreviate PPO with LSTM as PPO-LSTM.

Transformers

The transformer architecture, initially designed for sequence transduction tasks [51], has shown equal success in a variety of domains such as computer vision [10] and genomics [8]. Applying transformers to RL has been challenging, especially due to the instability they showed initially [33]. Pleines et al. [35] have successfully applied the TrXL architecture to memory tasks in RL. Unlike frame-stacking which provides fixed-window history or LSTMs which compress information through gating, transformers can attend to any part of the observation sequence [51]. While transformers have shown promise in partially observable sequential decision-making tasks, their application to penetration testing remains relatively unexplored compared to LSTM-based approaches. We use the implementation provided in the `cleanRL` repository [15].

4.3 Hyperparameter Tuning

Since this study involves a systematic comparison of different algorithms, we conduct a hyperparameter search for each algorithm, to enable a fair comparison. We use Optuna as our optimization framework [2]. The hyperparameters are sampled using Optuna’s Tree-structured Parzen Estimator (TPE) sampler, a Bayesian optimization method, which efficiently learns from previous trials to suggest promising hyperparameter combinations [4]. Every algorithm has been tuned with a budget of 250 trials. Each trial runs for a maximum of 5 million environment steps, though we employ Optuna’s Median Pruner to terminate unpromising trials early after the second evaluation. This pruning mechanism compares a trial’s intermediate performance against the median of previous trials around the same evaluation timestep. Importantly, we do not fix the seeds during the hyperparameter search. During the learning phase, the policy is evaluated at intervals of one million steps on freshly generated environments. Each evaluation consists of 100 episodes. The objective function maximizes the mean undiscounted cumulative reward across the 100 evaluation episodes. The full range of hyperparameters tested, along with the best-performing ones for each algorithm, are reported in Appendix A.

For tuning the hyperparameters of PPO, PPO-AO, PPO-FS and PPO-LSTM, we use the `rl-baselines3-zoo` library [37]. For PPO-TrXL, we wrote a hyperparameter-tuning script adhering to the same structure.

5 Experiments

5.1 Setup

Table 1 summarizes the StochNASim parameters most relevant to this analysis. We now provide justification for these parameter choices and discuss their impact on the learning environment.

Network Configuration: We configure networks to vary between 5 and 8 hosts to balance computational tractability with meaningful complexity variation. This range

Table 1: Environment parameters for StochNASim used throughout the hyperparameter tuning and experiments.

Min. Num. Hosts	5	Max. Num. Hosts	8
Exploit Success Prob.	0.9	Priv. Esc. Success Prob.	0.9
Exploit Cost	3	Priv. Esc. Cost	3
Host Value	5	Sensitive Host Value	100
Cost of Scans	1	Num. OSes	2
Num. Services	2	Num. Processes	2
Num. of Sensitive Hosts	2		

ensures that agents encounter networks of different sizes while maintaining reasonably sized action space and moderate episode lengths. Given the chosen parameters, the size of the action space (Section 4.1 equals 96.

Action Costs and Rewards: The cost structure in Table 1 reflects realistic penetration testing considerations. Scan actions (cost = 1) represent low-risk reconnaissance activities that are quick to execute but provide limited information. Exploit and privilege escalation actions (cost = 3) are more expensive, reflecting their higher computational overhead, increased detection risk, and potential for causing system disruption. The host value (5) provides modest rewards for gaining access, while sensitive hosts (value = 100) offer substantially higher rewards, creating a clear reward hierarchy that mirrors real-world target prioritization.

Success Probabilities: We set exploit and privilege escalation success probabilities to 0.9 rather than making them deterministic. We consider this more realistic as real-world exploits can fail due to factors like timing, system state, or defensive countermeasures. This stochasticity encourages learning more robust policies by exposing agents to occasional failures that must be recognized and retried.

Operating System and Service Diversity: We limit the environment to 2 operating systems, 2 services, and 2 processes per category. While this may seem restrictive compared to real-world diversity, it provides sufficient complexity for our comparative study while ensuring that hyperparameter tuning remains computationally feasible. This simplified setup allows us to focus on the core challenge of partial observability without being overwhelmed by combinatorial explosion of possible configurations.

Step Limit: The original NASim environment used a step limit of 1000 for networks of size 5 and 8. We chose to increase the step limit to 5000, to avoid making the problem artificially easier by discarding episodes too early [34]. The method employed to decide on this number was to run a random agent for 100,000 episodes in the environment. We then took the average number of steps required per episode and multiplied it by an order of magnitude and rounded it up.

5.2 Evaluating Hyperparameters

After establishing these environment parameters, we conducted hyperparameter optimization for each algorithm using the methodology established in Section 4.3. Following the hyperparameter search, we select, for each algorithm, the parameters that achieved the highest final evaluation score and assess their performance over a new training run across five control seeds, with a budget of 5 million steps. Using this set of control seeds, we aim to demonstrate the stability of learning and ensure that the selected hyperparameters are not overfit to a single seed. During training, we also evaluate the policy on separate, newly generated, environments at intervals of 500k steps for 100 episodes. We chose such a large amount of evaluation episodes to ac-

count for variable episode lengths across network sizes. This regular evaluation serves multiple purposes: it allows us to track training progress over time and validate that our selected hyperparameters lead to consistent improvement, rather than just achieving good final scores by chance. Fig. 3a showcases the training performance of the different algorithms in the form of learning curves. First, we observe that PPO-AO converges twice as fast as PPO-TrXL, and four times faster than the remaining methods, while achieving a larger cumulative reward. Second, PPO consistently reaches the end of the environment. Although it outperforms a random policy, demonstrating that the agent has acquired some task-relevant behaviour, PPO requires significantly more steps compared to the other methods, thus learning a policy we consider sub-optimal. It further underscores that solving a POMDP is markedly harder without a mechanism to integrate past observations. Fig. 3b shows the IQM Normalized Score achieved during the intermediary evaluations, plotted using the `rliable` [1] library for statistically robust performance comparison. Finally, Fig. 3c shows the mean number of steps, during the evaluation periods, required to complete the task of gaining root access on both sensitive hosts. What is notable from this plot is how close PPO-TrXL, PPO-AO and PPO-FS sit together. All three reach the end of an episode in 15-20 steps on average, with cumulative rewards between 140-180. The main takeaway from Fig. 3b and Fig. 3c is that while the top three algorithms reach a solution in roughly the same number of steps, they converge to distinct cumulative rewards, suggesting that their learned policies differ, which warrants a detailed analysis of the learned behaviour.

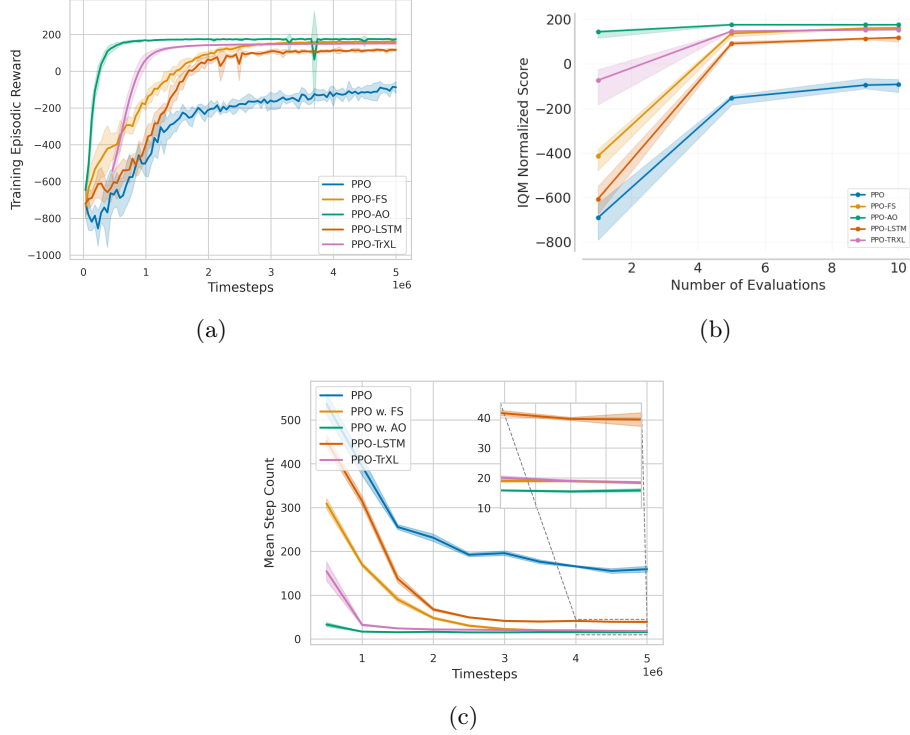


Figure 3: All results are aggregated over 5 seeds. (a) Learning curves of selected algorithms. (b) IQM Normalized Score achieved during intermediary policy evaluations on separate set of environments during training runs. (c) Mean step count to reach the end of a given scenario during intermediary policy evaluations.

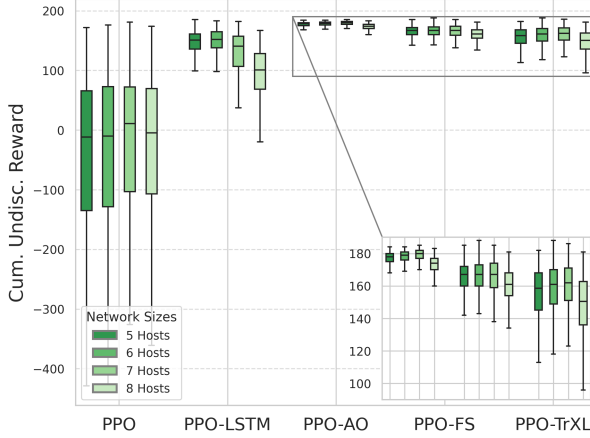


Figure 4: Performance sensitivity analysis across network sizes. Box plots show cumulative undiscounted reward distributions over 50 episodes per network size using the best-performing model from each algorithm. PPO-AO consistently outperforms other methods across all network sizes.

5.3 Evaluating Learned Policies

While the training curves provide insights into algorithm efficiency and convergence, they do not reveal the qualitative differences in the behaviours the agents learned. To gain further insights into how these policies actually operate we perform additional experiments. To start off, we look at the performance given specific network sizes, with the goal of investigating whether a larger network size has significant influence on the overall achieved reward. To assess performance by network size we load all trained models. Per algorithm we have five models, one for every evaluation seed. We then collect 50 episodes of data per network size. We visualize this data in one box plot per network size, per algorithm in Fig. 4. This plot gives us better insight into the variance of learned policies. We further confirm that PPO-AO was able to learn the best performing policies. We also observe that every algorithm, except PPO-LSTM, achieves its highest mean reward on networks composed of 7 hosts. We attribute this to the way the networks are generated (Section 4.1). With a maximum of 5 hosts per subnet and the DMZ and sensitive hosts occupying separate subnets, the 7th host's placement becomes highly predictable, as it consistently appears as the final host in the user subnet. The addition of an 8th host triggers the creation of an additional subnet, fundamentally altering the network topology. This predictable structure enables agents to develop effective heuristics, such as prioritizing the 7th host when identifying targets for the final two required exploits. Since our evaluation spans four network sizes (5–8 hosts), the 7th host represents the final host in 25% of all scenarios, making it a reliable target. In contrast, networks with 8 hosts introduce additional complexity that degrades performance across all algorithms except vanilla PPO. We attribute this behaviour to the high entropy of the policy, which is required due to not making use of any mechanism to handle the partial observability of the environment. PPO-LSTM experiences the most pronounced decline, showing difficulties to reliably navigate to further subnets.

Beyond performance differences, we also observe qualitative differences in the policies that the different algorithms learn. We showcase this in two ways. First, we analyse the action type distribution across a number of episodes. Second, we take a closer look at an action sequence by investigating the action being taken per timestep.

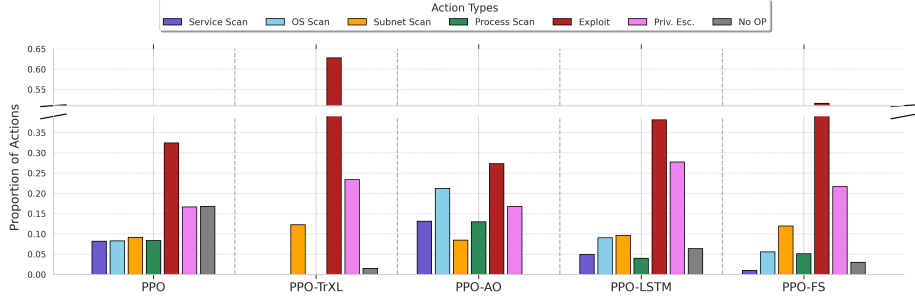


Figure 5: Action type distribution per algorithm, revealing distinct learned strategies despite similar performance outcomes. Data gathered over 50 episodes on separate environments

To create the action type distributions, we load the best overall model for each algorithm. This model was determined by evaluating which one achieves the highest mean reward over 100 episodes. The environment is seeded with the same seed for every algorithm which results in the same sequence of initial states when resetting the environment after every episode. This allows for a better and fairer comparison. With these models loaded, we again collect 50 episodes of data, consisting of the executed action, whether it was successful, and the obtained reward. Next, we compute the proportions for each action type. Fig. 5 reveals stark differences in learned policies. The most significant contrast is between PPO-TrXL and the other algorithms. PPO-TrXL appears to have learned no scanning behaviour, instead adopting a brute-force strategy to navigate the network. In contrast, we observe that PPO-AO spends most of its steps, compared to the other algorithms, on scan actions. PPO-FS sits somewhere between PPO-AO and PPO-TrXL, performing only a small amount of scanning, while over half of the actions are executing exploit actions. When examining PPO’s action distribution, we observe a fairly even spread across all action types. We interpret this as evidence of policy uncertainty stemming from the absence of any history-tracking mechanism. Without access to historical information, the agent cannot leverage prior observations to inform its decision-making, resulting in a highly stochastic policy that lacks the strategic focus demonstrated by methods with memory capabilities.

To explore the learned policies more thoroughly, we select one sequence out of the 50 collected episodes that’s representative of the performance of each algorithm, and plot a detailed breakdown of the action sequence in Fig. 6. This confirms the observation from Fig. 3, that while PPO-AO, PPO-FS, and PPO-TrXL achieved similar cumulative results, using a similar number of steps, they learned very different policies.

5.4 Stochasticity Analysis

Since NASim only allows learning on fixed-sized networks, we contribute a wrapper to enable fair comparison between environments. This wrapper generates four scenarios at the beginning, one for each network size (5-8), and then cycles through them during training. At each episode, we pick one of these four scenarios; unlike StochNASim, we reuse the same four scenarios rather than generating new ones. We perform five training runs over one millions total steps for each environment using PPO-AO, as discussed in Section 4.2. Each run at intervals of 100k, the policy is evaluated on a different set of network configurations. The hyperparameters can be found in Appendix A.

This experimental setup reveals striking differences in learning dynamics between

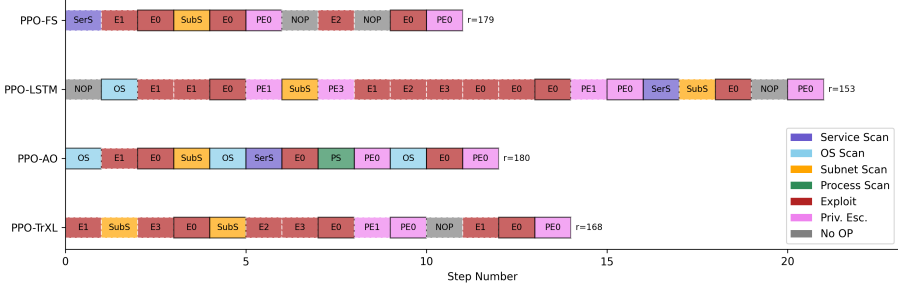


Figure 6: Representative action sequences on a 5-host network. Colours indicate action types, black outlines show success, dotted white show failures. Episode rewards ($r=X$) and lengths demonstrate strategy efficiency differences.

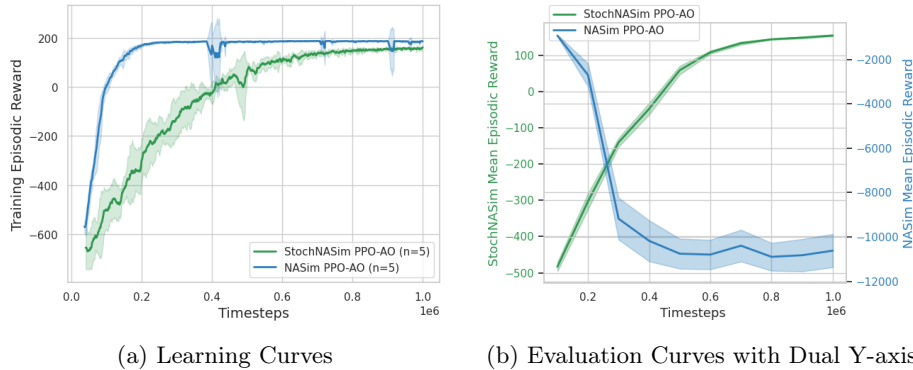


Figure 7: Training and evaluation performance comparison of PPO-AO trained StochNASim and NASim. Results aggregated over 5 seeds. Policies learned in NASim transfer poorly to unseen network configurations.

the two environments. Figure 7a shows that learning in NASim is simpler. We see less variance and the policy converges after 250k steps. In StochNASim, the policy requires the full training time to converge. This is expected, as in NASim, there are just four scenarios to learn. For StochNASim, on the other hand, we use an unbounded number of environments, and so the agent has to learn how to act in general, instead of learning an attack sequence by heart. This leads to a more robust policy that can easily be transferred and evaluated on a separate set of environments, as can be seen in Figure 7b. The policy learned on NASim transfers poorly to new scenarios, showing significantly degraded performance when facing novel network configurations.

6 Discussion

The experimental results highlight several important trends and insights. First, the use of StochNASim leads to the ability to generalize over many different generated networks, leading to robust policies that can easily be transferred between configurations, as shown by our experiments in Section 5.4. Second, within the selected algorithms, PPO-AO consistently achieved the highest performance, learning policies that efficiently balance information gathering and exploitation. Despite their architectural complexity, LSTM and transformer-based methods underperformed compared

to feedforward PPO variants, with PPO-TrXL notably avoiding scanning altogether. This is an important finding, especially for practical applications, considering the computational overhead that comes with training recurrent- and transformer-based architectures. Further, these findings raise important questions about what constitutes effective penetration testing policies in partially observable environments.

To interpret these results, we must first establish what characterizes effective penetration testing behaviour. An optimal policy should achieve the highest cumulative reward by eliminating the use of unnecessary actions, since all actions incur penalties, with exploit and privilege escalation actions incurring higher costs than scans. The optimal policy thus involves systematically gathering information through scans, retaining this information to avoid redundant scanning, and then selecting the appropriate exploit or privilege escalation action based on the gathered intelligence.

A key finding of our study is that the nature of this task does not require complex nor computationally expensive approaches such as LSTM or transformer architectures. Given the information-retrieval nature of the environment, simply encoding observation history as augmented inputs proves highly effective. This approach allows the agent to learn a policy that carefully gathers the necessary information and acts on it efficiently, much like a human penetration tester would approach the task: methodically collecting and evaluating information before selecting the right exploit to launch.

Interestingly, our manual inspection of learned policies reveals distinct behavioural patterns among the policies learnt by the different algorithms we studied. PPO-TrXL learned a brute-force policy, sequentially trying every exploit until gaining user access, then attempting every privilege escalation action until achieving root access. PPO-LSTM does make use of scans, but overall, the LSTM architecture was not able to learn a good representation of the history. Requiring almost twice the amount of steps to exploit all the sensitive hosts. PPO-FS demonstrated more refined behaviour, learning to match privilege escalation actions to discovered information but still executing exploits sequentially. Only PPO-AO achieved what we consider an optimal policy, executing the task efficiently with minimal redundant actions.

These results highlight a crucial insight: not tracking the observation history leads to significantly worse policies that would be impractical in real-world environments. However, the solution need not be computationally expensive: simple observation augmentation outperforms sophisticated memory architectures for this particular domain.

Looking towards future work, a key limitation of our current approach becomes apparent in more realistic settings, such as dynamic network environments where host states can change during an episode. These changes may include hosts shutting down, firewall rules being updated, or paths becoming unavailable, which can render previously collected observations invalid. In such cases, hand-crafted observation augmentations might become brittle and infeasible to maintain. Moreover, in many real-world scenarios, it is impractical or intractable to design augmentations manually. Ideally, we would rely on the agent itself to learn effective state representations that integrate relevant historical information and adapt to evolving conditions. Architectures such as LSTMs and transformers are designed to support such functionality by learning from sequences directly, but our empirical results show that their performance remains limited in this context. This suggests that these models may be struggling to capture the specific type of memory, reasoning, or structural understanding required for effective decision-making in partially observable and dynamic environments. An interesting avenue for future work lies in developing or adapting history aware models, with stronger inductive biases or explicit memory mechanisms, that can better handle such evolving, partially observed domains.

7 Conclusion

In this work, we modelled penetration testing as a partially observable sequential decision-making problem in stochastic environments encompassing networks of varying sizes. To address the limitations of existing simulators that use fixed network configurations, we developed StochNASim, a stochastic extension of NASim that generates new network topologies with varying host properties and network sizes for each episode. Using this environment, we systematically compared different approaches for addressing partial observability, ranging from no memory mechanism (baseline) to augmented observations, frame-stacking, LSTM, and transformers. Our findings reveal that this task is well-suited for simpler memory mechanisms that track observation history through direct aggregation. Interestingly, complex architectures like LSTMs and transformers failed to learn sophisticated policies, instead developing undesirable brute-force approaches that sequentially attempt all possible actions. Notably, PPO-AO outperformed all other methods, learning the most efficient and human-like penetration testing strategies while converging three times faster than competing approaches. The stochastic nature of StochNASim proved crucial for developing robust policies. Our comparison between fixed and stochastic environments demonstrated that policies trained on static configurations show poor generalization to novel scenarios, while those trained in our variable environment maintain consistent performance across different network configurations. This highlights the importance of stochastic training environments for learning policies applicable to real-world penetration testing scenarios. Crucially, our results demonstrate the importance of looking beyond learning curves and final rewards when evaluating learned policies. We found that algorithms achieving similar quantitative performance can learn vastly different behavioural strategies, highlighting the value of qualitative policy analysis in understanding algorithmic effectiveness. While our experiments were conducted in simulation, these insights are particularly relevant as the field moves toward real-world penetration testing applications, where efficient, interpretable, reliable and robust policies are essential for practical deployment.

Acknowledgment

This research was supported by funding from the Flemish Government under the “Onderzoeksprogramma Artificiële Intelligentie (AI) Vlaanderen” program. The resources and services used in this work were, in part, provided by the VSC (Flemish Supercomputer Center), funded by the Research Foundation - Flanders (FWO) and the Flemish Government. Pieter Libin acknowledges support from the Research council of the Vrije Universiteit Brussel (OZR-VUB) via grant number OZR3863BOF. We also thank Florent Delgrange and Raphael Avalos for their invaluable insights, Mehrdad Asadi for feedback on visualizations and Arbia Riahi for proof reading.

References

- [1] R. Agarwal, M. Schwarzer, P. S. Castro, A. C. Courville, and M. Bellemare. Deep reinforcement learning at the edge of the statistical precipice. *Advances in neural information processing systems*, 34:29304–29320, 2021.
- [2] T. Akiba, S. Sano, T. Yanase, T. Ohta, and M. Koyama. Optuna: A next-generation hyperparameter optimization framework. In *The 25th ACM SIGKDD International Conference on Knowledge Discovery & Data Mining*, pages 2623–2631, 2019.
- [3] R. Avalos, F. Delgrange, A. Nowe, G. Perez, and D. M. Roijers. The wasserstein believer: Learning belief updates for partially observable environments through

reliable latent space models. In *The Twelfth International Conference on Learning Representations*, 2024.

- [4] J. Bergstra, R. Bardenet, Y. Bengio, and B. Kégl. Algorithms for hyper-parameter optimization. *Advances in neural information processing systems*, 24, 2011.
- [5] C. Berner, G. Brockman, B. Chan, V. Cheung, P. Dębiak, C. Dennison, D. Farhi, Q. Fischer, S. Hashme, C. Hesse, et al. Dota 2 with large scale deep reinforcement learning. *arXiv preprint arXiv:1912.06680*, 2019.
- [6] K. Cobbe, C. Hesse, J. Hilton, and J. Schulman. Leveraging procedural generation to benchmark reinforcement learning. In *Proceedings of the 37th International Conference on Machine Learning*, ICML’20. JMLR.org, 2020.
- [7] K. Cobbe, O. Klimov, C. Hesse, T. Kim, and J. Schulman. Quantifying generalization in reinforcement learning. In *International conference on machine learning*, pages 1282–1289. PMLR, 2019.
- [8] M. E. Consens, C. Dufault, M. Wainberg, D. Forster, M. Karimzadeh, H. Goodarzi, F. J. Theis, A. Moses, and B. Wang. Transformers and genome language models. *Nature Machine Intelligence*, pages 1–17, 2025.
- [9] J. Degrave, F. Felici, J. Buchli, M. Neunert, B. Tracey, F. Carpanese, T. Ewalds, R. Hafner, A. Abdolmaleki, D. de Las Casas, et al. Magnetic control of tokamak plasmas through deep reinforcement learning. *Nature*, 602(7897):414–419, 2022.
- [10] A. Dosovitskiy, L. Beyer, A. Kolesnikov, D. Weissenborn, X. Zhai, T. Unterthiner, M. Dehghani, M. Minderer, G. Heigold, S. Gelly, et al. An image is worth 16x16 words: Transformers for image recognition at scale. *arXiv preprint arXiv:2010.11929*, 2020.
- [11] G. Dulac-Arnold, N. Levine, D. J. Mankowitz, J. Li, C. Paduraru, S. Gowal, and T. Hester. Challenges of real-world reinforcement learning: definitions, benchmarks and analysis. *Machine Learning*, 110(9):2419–2468, 2021.
- [12] D. Ghosh, J. Rahme, A. Kumar, A. Zhang, R. P. Adams, and S. Levine. Why generalization in rl is difficult: Epistemic pomdps and implicit partial observability. *Advances in neural information processing systems*, 34:25502–25515, 2021.
- [13] M. Hausknecht and P. Stone. Deep Recurrent Q-Learning for Partially Observable MDPs, Jan. 2017. *arXiv:1507.06527 [cs]*.
- [14] S. Hochreiter and J. Schmidhuber. Long short-term memory. *Neural computation*, 9(8):1735–1780, 1997.
- [15] S. Huang, R. F. J. Dossa, C. Ye, J. Braga, D. Chakraborty, K. Mehta, and J. G. Araújo. Cleanrl: High-quality single-file implementations of deep reinforcement learning algorithms. *Journal of Machine Learning Research*, 23(274):1–18, 2022.
- [16] F. Hutter, H. Hoos, and K. Leyton-Brown. An efficient approach for assessing hyperparameter importance. In *Proceedings of the 31st International Conference on Machine Learning*, volume 32, pages 754–762, Beijing, China, 22–24 Jun 2014. PMLR.
- [17] R. T. Icarte, T. Q. Klassen, R. Valenzano, and S. A. McIlraith. Reward machines: Exploiting reward function structure in reinforcement learning. *Journal of Artificial Intelligence Research*, 73:173–208, 2022.
- [18] ISC². Cybersecurity workforce study. 2023.
- [19] J. Janisch, T. Pevný, and V. Lisý. NASimEmu: Network Attack Simulator & Emulator for Training Agents Generalizing to Novel Scenarios, Aug. 2023. *arXiv:2305.17246 [cs]*.
- [20] L. P. Kaelbling, M. L. Littman, and A. R. Cassandra. Planning and acting in partially observable stochastic domains. *Artificial intelligence*, 101(1-2):99–134, 1998.

- [21] Q. Li, M. Hu, H. Hao, M. Zhang, and Y. Li. INNES: An intelligent network penetration testing model based on deep reinforcement learning. *Applied Intelligence*, 53(22):27110–27127, Nov. 2023.
- [22] Q. Li, R. Wang, D. Li, F. Shi, M. Zhang, and A. Chattopadhyay. Dynpen: Automated penetration testing in dynamic network scenarios using deep reinforcement learning. *IEEE Transactions on Information Forensics and Security*, 2024.
- [23] Y. Li, H. Dai, and J. Yan. Knowledge-informed auto-penetration testing based on reinforcement learning with reward machine. In *2024 International Joint Conference on Neural Networks (IJCNN)*, pages 1–9. IEEE, 2024.
- [24] Z. Li, Q. Zhang, and G. Yang. EPPTA: Efficient partially observable reinforcement learning agent for penetration testing applications. n/a:e12818. _eprint: <https://onlinelibrary.wiley.com/doi/pdf/10.1002/eng2.12818>.
- [25] M. C. Libicki, L. Ablon, and T. Webb. *The Defender’s Dilemma: Charting a Course Toward Cybersecurity*. Number RR-1024-JNI in Research Report. RAND Corporation, 2015. Accessed: May 21, 2025.
- [26] P. J. Libin, A. Moonens, T. Verstraeten, F. Perez-Sanjines, N. Hens, P. Lemey, and A. Nowé. Deep reinforcement learning for large-scale epidemic control. In *European Conference in Machine Learning 2020, Ghent, Belgium*, pages 155–170. Springer, 2021.
- [27] T. Macaulay. The danger of critical infrastructure interdependency. *Centre for International Governance Innovation*, 2019. Accessed: May 21, 2025.
- [28] V. Mnih, K. Kavukcuoglu, D. Silver, A. A. Rusu, J. Veness, M. G. Bellemare, A. Graves, M. Riedmiller, A. K. Fidjeland, G. Ostrovski, et al. Human-level control through deep reinforcement learning. *Nature*, 518(7540):529–533, 2015.
- [29] National Institute of Standards and Technology. Technical guide to information security testing and assessment. Technical Report SP 800-115, NIST, September 2008.
- [30] National Institute of Standards and Technology. Assessing security and privacy controls in information systems and organizations. Technical Report SP 800-53A Rev. 5, NIST, 2022.
- [31] T. Ni, B. Eysenbach, and R. Salakhutdinov. Recurrent Model-Free RL Can Be a Strong Baseline for Many POMDPs. In *Proceedings of the 39th International Conference on Machine Learning*, pages 16691–16723. PMLR, June 2022. ISSN: 2640-3498.
- [32] S. Oesch, A. Chaulagain, B. Weber, M. Dixson, A. Sadovnik, B. Roberson, C. Watson, and P. Austria. Towards a high fidelity training environment for autonomous cyber defense agents. In *Proceedings of the 17th Cyber Security Experimentation and Test Workshop, CSET ’24*, pages 91–99. Association for Computing Machinery, 2024.
- [33] E. Parisotto, F. Song, J. Rae, R. Pascanu, C. Gulcehre, S. Jayakumar, M. Jaderberg, R. L. Kaufman, A. Clark, S. Noury, et al. Stabilizing transformers for reinforcement learning. In *International conference on machine learning*, pages 7487–7498. PMLR, 2020.
- [34] A. Patterson, S. Neumann, M. White, and A. White. Empirical design in reinforcement learning. *Journal of Machine Learning Research*, 25(318):1–63, 2024.
- [35] M. Pleines, M. Pallasch, F. Zimmer, and M. Preuss. Memory gym: Towards endless tasks to benchmark memory capabilities of agents. *Journal of Machine Learning Research*, 26(6):1–40, 2025.

[36] M. L. Puterman. Chapter 8 markov decision processes. In *Stochastic Models*, volume 2 of *Handbooks in Operations Research and Management Science*, pages 331–434. Elsevier, 1990.

[37] A. Raffin. Rl baselines3 zoo. <https://github.com/DLR-RM/rl-baselines3-zoo>, 2020.

[38] A. Raffin, A. Hill, A. Gleave, A. Kanervisto, M. Ernestus, and N. Dormann. Stable-baselines3: Reliable reinforcement learning implementations. *Journal of Machine Learning Research*, 22(268):1–8, 2021.

[39] Q. Ren, J. Liu, X. Xiong, and C. Lu. Automated penetration testing based on lstm and advanced curiosity exploration. In *2024 IEEE 5th International Conference on Pattern Recognition and Machine Learning (PRML)*, pages 150–156. IEEE, 2024.

[40] C. Sarraute, O. Buffet, and J. Hoffmann. Penetration Testing == POMDP Solving?, June 2013. arXiv:1306.4714 [cs].

[41] J. Schulman, S. Levine, P. Abbeel, M. Jordan, and P. Moritz. Trust region policy optimization. In *International conference on machine learning*, pages 1889–1897. PMLR, 2015.

[42] J. Schulman, F. Wolski, P. Dhariwal, A. Radford, and O. Klimov. Proximal Policy Optimization Algorithms, Aug. 2017. arXiv:1707.06347 [cs].

[43] J. Schwartz and H. Kurniawatti. Nasim: Network attack simulator. <https://networkattacksimulator.readthedocs.io/>, 2019.

[44] D. Silver, J. Schrittwieser, K. Simonyan, I. Antonoglou, A. Huang, A. Guez, T. Hubert, L. Baker, M. Lai, A. Bolton, et al. Mastering the game of go without human knowledge. *nature*, 550(7676):354–359, 2017.

[45] M. Standen, M. Lucas, D. Bowman, T. J. Richer, J. Kim, and D. Marriott. CybORG: A Gym for the Development of Autonomous Cyber Agents, Aug. 2021. arXiv:2108.09118 [cs].

[46] B. E. Strom, A. Applebaum, D. P. Miller, K. C. Nickels, A. G. Pennington, and C. B. Thomas. Mitre att&ck: Design and philosophy. In *Technical report*. The MITRE Corporation, 2018.

[47] R. S. Sutton and A. G. Barto. *Reinforcement Learning: An Introduction*. A Bradford Book, Cambridge, MA, USA, 2018.

[48] M. D. R. Team. Cyberbattlesim. <https://github.com/microsoft/cyberbattlesim>, 2021. Created by Christian Seifert, Michael Betser, William Blum, James Bono, Kate Farris, Emily Goren, Justin Grana, Kristian Holsheimer, Brandon Marken, Joshua Neil, Nicole Nichols, Jugal Parikh, Haoran Wei.

[49] F. Terranova, A. Lahmadi, and I. Chrisment. Leveraging deep reinforcement learning for cyber-attack paths prediction: Formulation, generalization, and evaluation. In *Proceedings of the 27th International Symposium on Research in Attacks, Intrusions and Defenses*, pages 1–16, 2024.

[50] K. Tran, M. Standen, J. Kim, D. Bowman, T. Richer, A. Akella, and C.-T. Lin. Cascaded Reinforcement Learning Agents for Large Action Spaces in Autonomous Penetration Testing. *Applied Sciences*, 12(21):11265, Jan. 2022. Number: 21 Publisher: Multidisciplinary Digital Publishing Institute.

[51] A. Vaswani, N. Shazeer, N. Parmar, J. Uszkoreit, L. Jones, A. N. Gomez, L. Kaiser, and I. Polosukhin. Attention is all you need. *Advances in neural information processing systems*, 30, 2017.

[52] R. J. Williams. Simple statistical gradient-following algorithms for connectionist reinforcement learning. *Machine learning*, 8:229–256, 1992.

- [53] World Economic Forum. Global cybersecurity outlook 2023. *Insight Report*, 2023.
- [54] Y. Yang and X. Liu. Behaviour-Diverse Automatic Penetration Testing: A Curiosity-Driven Multi-Objective Deep Reinforcement Learning Approach, Feb. 2022. arXiv:2202.10630 [cs].
- [55] C. Zhang, O. Vinyals, R. Munos, and S. Bengio. A study on overfitting in deep reinforcement learning. *arXiv preprint arXiv:1804.06893*, 2018.
- [56] Y. Zhang, J. Liu, S. Zhou, D. Hou, X. Zhong, and C. Lu. Improved Deep Recurrent Q-Network of POMDPs for Automated Penetration Testing. *Applied Sciences*, 12(20):10339, Jan. 2022. Number: 20 Publisher: Multidisciplinary Digital Publishing Institute.
- [57] S. Zhou, J. Liu, D. Hou, X. Zhong, and Y. Zhang. Autonomous Penetration Testing Based on Improved Deep Q-Network. *Applied Sciences*, 11(19):8823, Jan. 2021. Number: 19 Publisher: Multidisciplinary Digital Publishing Institute.

Table 2: Hyperparameter search ranges for PPO, PPO-FS and PPO-AO. Best performing parameter values for PPO are marked in **bold**, underlined for PPO-FS and in *italics* for PPO-AO.

Hyperparameter	Values
Batch Size	64, <u>128</u> , 256 , <u>512</u>
Number of Steps	128, 256, 512, 1024 , <u>2048</u>
Discount Factor (γ)	0.95, 0.97 , 0.99, 0.995, <u>0.999</u>
Learning Rate	3e-5, 1e-4, <i>3e-4</i> , <u>1e-3</u> , 3e-3
Entropy Coefficient	1e-3, 5e-3, <u>1e-2</u> , 5e-2, 1e-1
Clip Range	0.1, <u>0.2</u> , 0.3, 0.4
Number of Epochs	<u>5</u> , <i>10</i> , 20
GAE Lambda	0.9 , <u>0.95</u> , 0.99
Maximum Gradient Norm	0.5, 0.6 , 0.7, 0.8, 0.9, <u>1</u> , 2
Value Function Coefficient	0.3 , <u>0.5</u> , 0.7
<i>Network Parameters</i>	
Activation Function	tanh , <u>ReLU</u>
Orthogonal Initialization	False (fixed)
Network Architecture	Tiny: $\pi=[64]$, $vf=[64]$ Small: $\pi=[64, 64]$, $vf=[64, 64]$ Medium: $\pi=[128, 128]$, $vf=[128, 128]$ Large : $\pi=[256]$, $vf=[256]$ Very large: $\pi=[256, 256]$, $vf=[256, 256]$
<i>PPO-FS specific parameters</i>	
Frame Stack	4, <u>8</u> , 16, 32

A Hyperparameters

For PPO-TrXL, we've taken most of the hyperparameter ranges from the original implementation as they are described the the work of Pleines et. al [35]. Some modification have been made to the number of steps performed per rollout and the number of environments use. We used 768 steps per rollout and 8 environments. This choice stems from memory restrictions on the GPUs that we used. PPO-TrXL was trained on a cluster of four NVIDIA A100 and H100 respectively. When testing the implementation, we found that not collecting enough steps from the environment may result in unfinished episodes, which will terminate the training because there is no data to bootstrap on. The remaining algorithms have been trained on a clusters composed of Intel Xeon Gold 6148 (Skylake). Tables 2–4 showcase the hyperparameter ranges that were used during the search initially described in Section 4.3.

A.1 Sensitivity Analysis

Fig. 8 showcases the importances of the different hyperparameters for each algorithm established in Section 4.2. We can see that for PPO without any history aggregation or reconstruction, the most important parameter is the entropy coefficient. It controls to which degree the policy is going to pick random actions, instead of the best one. The entropy accounts for half of the total variability of the trials. This reflects an inherent uncertainty that is present, since the decision which action to take solely relies on the last observation. When comparing the importances for PPO to frame-stacking

Table 3: Hyperparameter search ranges for PPO-LSTM optimization. Best performing parameter values are marked in **bold**.

Hyperparameter	Values
Batch Size	64, 128, 256, 512
Number of Steps	128, 256, 512 , 1024, 2048
Discount Factor (γ)	0.99 , 0.995, 0.999
Learning Rate	1e-5, 3e-5, 1e-4, 3e-4, 1e-3
Entropy Coefficient	1e-3, 5e-3, 1e-2, 5e-2 , 1e-1
Clip Range	0.1 , 0.2, 0.3, 0.4
Number of Epochs	5 , 10, 20
GAE Lambda	0.9, 0.95 , 0.98
Maximum Gradient Norm	0.5, 0.6, 0.7, 0.8, 0.9 , 1, 2
Value Function Coefficient	0.3 , 0.5, 0.7
<i>Network Parameters</i>	
Activation Function	tanh , ReLU
Orthogonal Initialization	False (fixed)
LSTM Hidden Size	64, 128 , 256
Enable Critic LSTM	True, False
Network Architecture	Small: $\pi=[64, 64]$, $vf=[64, 64]$ Medium: $\pi=[128, 128]$, $vf=[128, 128]$ Large : $\pi=[256]$, $vf=[256]$

Table 4: Hyperparameter search ranges for PPO-TrXL. Best performing parameter values are marked in **bold**.

Hyperparameter	Values
Number Mini Batches	2, 3, 4
Update Epochs	2, 3, 4
Discount Factor (γ)	0.95, 0.99, 0.995 , 0.999
Learning Rate init.	2e-4 , 2.75e-4, 3e-4, 3.5e-4
Learning Rate final (fixed)	1e-5
Entropy Coef. init.	1e-4 , 1e-3, 1e-2
Entropy Coef. final (fixed)	1e-6
Anneal Steps (fixed)	4020000
Clip Range	0.1 , 0.2, 0.3
Normalize Advantage	True, False
GAE Lambda (λ)	0.9, 0.95 , 0.99
Maximum Gradient Norm	0.25, 0.35, 0.5 , 1
Value Function Coefficient	0.2, 0.3 , 0.5
<i>TrXL Parameters</i>	
TrXL Num. Layers	2, 3, 4
TrXL Num. Heads	1 , 4, 8
TrXL Dimension	128, 256 , 384
TrXL Memory Length	128, 256, 512
Positional Encoding	none , absolute, learned

and the augmented observations, we can see that the entropy coefficient matters a lot less. This is due to more context provided in the observations, which helps creating a representation and therefore requiring less randomness from policy. They can better rely on the observations they receive. Something else that is worth highlighting is the importance of the number of stacked frames (or rather observations in our case) for PPO-FS. We would assume that the frame-stack parameter f_n played a more important role, but it accounts for less than 5% of the total variability. We interpret it that already a small amount of stacked observations are beneficial to enhance the overall performance. Interestingly, for PPO-TrXL, none of the TrXL architecture specific parameters appear to be the most important ones. Concerning PPO-LSTM, the batch size appears to be the most important parameter, accounting for approximately 35% of the total variability. This finding aligns with the unique challenges of training recurrent networks in reinforcement learning settings. Unlike the other PPO variants, LSTM networks require careful management of sequential dependencies and hidden state propagation across time steps. The batch size directly influences how many independent sequences the LSTM processes simultaneously, which is crucial for stable gradient estimation and proper learning of temporal patterns.

B Additional Notes on Experiments

The seeds that have been used in Section 5.2 are the following: 8258, 710, 6930, 8829, 7602. We simply pass them as an argument (`-seed`) to the scripts from `cleanRL` and `stable-baselines3`. The specific version we used for the `stable-baselines3` framework is 2.4. This holds for both the algorithm implementations as well as their hyperparameter tuning framework in `r1-baselines3-zoo`. The seed we employed for the environments regarding the experiments conducted in Section 5.3 is 2.

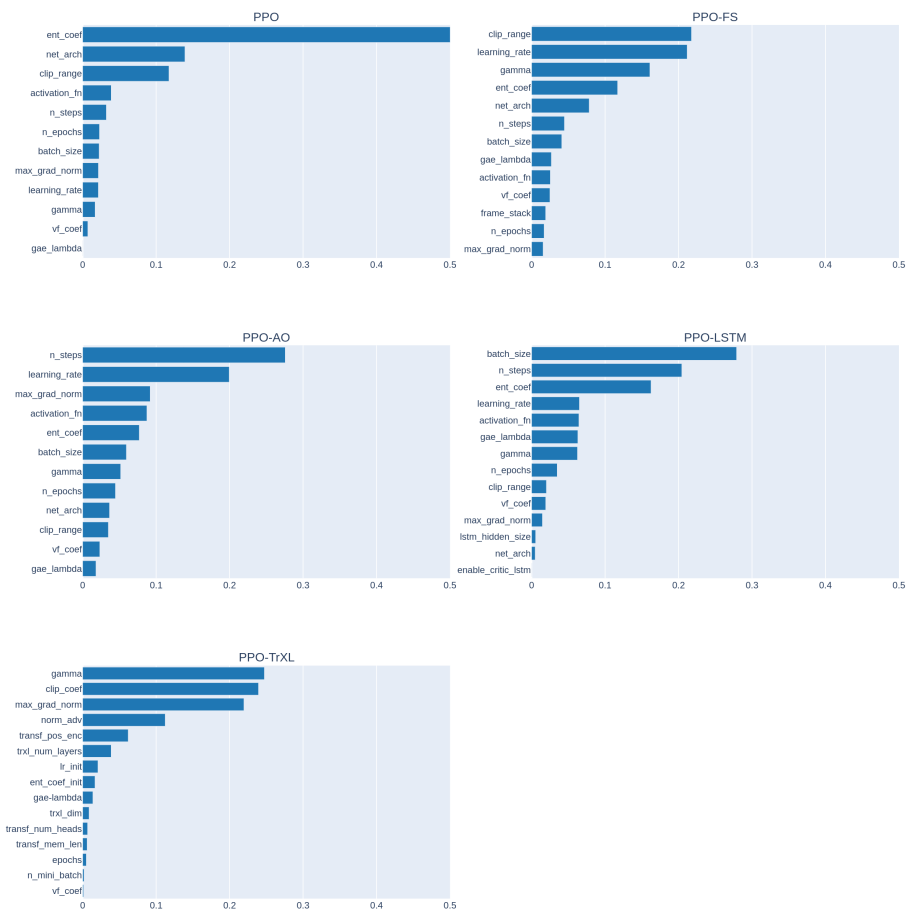


Figure 8: Hyperparameter importance analysis using fANOVA framework [16]. Values show the fraction of performance variance explained by each parameter across 250 optimization trials per algorithm.